Biochemical and Biophysical Research Communications 465 (2015) 12–18

Contents lists available at ScienceDirect

Biochemical and Biophysical Research Communications

journal homepage: www.elsevier.com/locate/ybbrc

Structural basis for the ligand-binding specificity of fatty acid-binding proteins (pFABP4 and pFABP5) in gentoo penguin

Chang Woo Lee [a, b], Jung Eun Kim [a, e], Hackwon Do [a], Ryeo-Ok Kim [a, 1], Sung Gu Lee [a, b], Hyun Ho Park [c], Jeong Ho Chang [d], Joung Han Yim [a], Hyun Park [a, b], Il-Chan Kim [a, **], Jun Hyuck Lee [a, b, *]

[a] Division of Polar Life Sciences, Korea Polar Research Institute, Incheon 406-840, Republic of Korea
[b] Department of Polar Sciences, University of Science and Technology, Incheon 406-840, Republic of Korea
[c] Department of Biochemistry, School of Biotechnology and Graduate School of Biochemistry, Yeungnam University, Gyeongsan, Republic of Korea
[d] Department of Biology Education, Kyungpook National University, Daegu 702-701, Republic of Korea
[e] Department of Pharmacy, Graduate School, Sungkyunkwan University, Suwon 440-746, Republic of Korea

ARTICLE INFO

Article history:
Received 7 July 2015
Accepted 17 July 2015
Available online 20 July 2015

Keywords:
Fatty acid-binding protein
β-barrel protein
Crystal structure
Gentoo penguin (*Pygoscelis papua*)
X-ray crystallography

ABSTRACT

Fatty acid-binding proteins (FABPs) are involved in transporting hydrophobic fatty acids between various aqueous compartments of the cell by directly binding ligands inside their β-barrel cavities. Here, we report the crystal structures of ligand-unbound pFABP4, linoleate-bound pFABP4, and palmitate-bound pFABP5, obtained from gentoo penguin (*Pygoscelis papua*), at a resolution of 2.1 Å, 2.2 Å, and 2.3 Å, respectively. The pFABP4 and pFABP5 proteins have a canonical β-barrel structure with two short α-helices that form a cap region and fatty acid ligand binding sites in the hydrophobic cavity within the β-barrel structure. Linoleate-bound pFABP4 and palmitate-bound pFABP5 possess different ligand-binding modes and a unique ligand-binding pocket due to several sequence dissimilarities (A76/L78, T30/M32, underlining indicates pFABP4 residues) between the two proteins. Structural comparison revealed significantly different conformational changes in the β3–β4 loop region (residues 57–62) as well as the flipped Phe60 residue of pFABP5 than that in pFABP4 (the corresponding residue is Phe58). A ligand-binding study using fluorophore displacement assays shows that pFABP4 has a relatively strong affinity for linoleate as compared to pFABP5. In contrast, pFABP5 exhibits higher affinity for palmitate than that for pFABP4. In conclusion, our high-resolution structures and ligand-binding studies provide useful insights into the ligand-binding preferences of pFABPs based on key protein–ligand interactions.

1. Introduction

Water insoluble fatty acids are a major component of the cell membranes as well as signaling molecules, and are transported between cellular organelles by selectively binding to fatty acid-binding proteins (FABPs). Nine types of FABP coding genes have been identified and named after the human tissue in which they are predominantly expressed: FABP1 (liver), FABP2 (intestine), FABP3 (heart), FABP4 (adipocytes), FABP5 (epidermis), FABP6 (ileum), FABP7 (brain), FABP8 (myelin), and FABP9 (testes) [1–3]. However, recent studies have shown that there is not only significant overlap in the tissue distribution of some members but these proteins also share high sequence homology (44–80%). Nevertheless, individual FABPs have specific ligand preferences and unique ligand-binding mechanisms [4].

Structures of several FABP proteins from various sources including human, mouse, chicken, and zebra fish are known [5–9]. Most FABP structures comprise primarily of 10-stranded β-barrels and two short α-helixes [1,10]. One end of the β-barrel is blocked by two short α-helixes, forming a capping structure. Inside the β-barrel is hydrophobic cavity that contains the fatty acid binding site. This structure has no channels large enough to allow fatty acids to enter or exit [11]. This suggests that ligand binding and release from FABPs would require significant conformational changes.

* Corresponding author. Division of Polar Life Sciences, Korea Polar Research Institute, Incheon 406-840, Republic of Korea.
** Corresponding author.
E-mail addresses: ickim@kopri.re.kr (I.-C. Kim), junhyucklee@kopri.re.kr (J.H. Lee).
[1] Current affiliation: Department of Biological Sciences, College of Science, Sungkyunkwan University, Suwon 440-746, Republic of Korea.

http://dx.doi.org/10.1016/j.bbrc.2015.07.087
0006-291X/

Notably, recent studies have shown that the ligand-bound human FABP5 structure is a domain swapped dimer [7]. This suggests that ligand binding might induce a conformational transition and change the oligomerization state from a monomer into a dimer. However, the binding mechanism and specificity of FABP ligands is even less well understood. The "flexibility in the portal region (between α2 helix and the α2-β2 linker)" model, proposes that a conformational change upon ligand binding is the possible driving force allowing ligands to enter and exit the hydrophobic protein cavity via a diffusion-based mechanism on the target membrane [12–14].

Studies focusing on the ligand-binding stoichiometry of FABP have shown that most FABPs have one ligand-binding site, except human FABP1, which is proposed to have two or even three fatty acid binding sites [15]. Further, the cavity size in FABP1 is speculated to be larger than other members of the FABP family. All FABPs contain a conserved arginine side chain, water molecules inside their β-barrel and a conserved fatty acid binding site. An ionic interaction between the FABP fatty acid binding site and the carboxyl terminus of the fatty acids appears to be largely responsible for the common positioning of fatty acids in different FABPs [16]. FABP4 and FABP5 are known to have selective interactions with nuclear receptors PPARγ and PPARβ, respectively, and they transfer the bound fatty acids to their nuclear receptor-binding partners. The fatty acid-bound PPARs are the active form of these proteins, and exhibit enhanced transcriptional activity [17–19].

In this study, we determined the three-dimensional structure and ligand binding properties of ligand unbound-pFABP4, linoleate-complexed pFABP4, and palmitate-complexed pFABP5 that were obtained from gentoo penguin (*Pygoscelis papua*) [20,21]. These high-resolution structures, together with ligand-binding studies, provide useful insights into the ligand recognition mechanism and ligand-binding preferences of pFABPs.

2. Material and methods

2.1. Cloning, expression, and purification of pFABPs

Full-length genes of pFABP4 (GenBank KR054393) and pFABP5 (GenBank KR054394) were amplified by polymerase chain reaction (PCR) using the cDNA template of *P. papua*. Primers used for PCR amplification of pFABP4 were: forward primer 5′-GCCATATGTGCGACCAGTTTGTGGGC-3′ and reverse primer 5′-GTGCTCGAGTCATGCTCTTTCGTAAACT-3′. Primers for PCR amplification of pFABP5 were: forward primer 5′-GCCATATGGCCATCGACGCGTTTTTAG-3′ and reverse primer 5′-GTGCTCGAGTCATGCCTTCTGGTAGACTC-3′. The amplified DNA fragments were cleaved with NdeI and XhoI restriction enzymes and ligated into the multi-cloning site (MCS) of the pET-28a vector (Novagen, Madison, USA). A hexa-histidine tag and a thrombin protease recognition site were added to the N-terminus of the final construct. After confirming the sequence, *Escherichia coli* strain BL21(DE3) was transformed by the pFABP4 vectors for protein expression. The cells were grown in 4 L of Luria–Bertani [26] medium supplemented with kanamycin (50 μg/ml) at 37 °C. When OD600 approached 0.7, expression was induced with 1.0 mM isopropyl-1-thio-β-D-galactopyranoside (IPTG) at 25 °C for 20 h. Cells were harvested by centrifugation (VS-24SMTi; Vision Scientific, Bucheon, Republic of Korea) at 7000 rpm and 4 °C for 20 min, and resuspended it in lysis buffer (50 mM sodium phosphate, 300 mM NaCl, 5 mM imidazole pH 8.0) with 0.2 mg/ml lysozyme and 0.6 mM phenylmethylsulfonyl fluoride (PMSF). Cells were lysed by sonication for 30 min on ice. Cell debris was removed by centrifugation of the lysate at 16,000 rpm for 1 h at 4 °C, and the clarified supernatant was poured into a gravity-flow column pre-packed with Ni-NTA resin (Qiagen, Hilden, Germany). The unbound protein flowed through, while the poly-histidine tag-fused pFABP4 remained bound to the Ni-NTA resin. This was followed by washes with 10 bed column volumes of wash buffer (50 mM sodium phosphate, 300 mM NaCl, 20 mM imidazole pH 8.0). The pFABP4 proteins were eluted with elution buffer (50 mM sodium phosphate, 300 mM NaCl, 300 mM imidazole pH 8.0), and the concentration of pFABP4 was determined using Amicon Ultra Centrifugal Filters (Ultracel-3K; Millipore, Darmstadt, Germany). The poly-histidine tag was cleaved with thrombin, incubated overnight at 4 °C, and then applied onto a Superdex 200 column (GE Healthcare, Piscataway, USA) equilibrated with 20 mM Tris–HCl (pH 8.0) and 150 mM NaCl. The fractions containing putative pFABP4 were collected and concentrated to 27.9 mg/ml by ultrafiltration using Amicon Ultra Centrifugal Filters. The pFABP5 was also expressed and purified as described above. The final concentration of purified pFABP5 was 54.1 mg/ml.

2.2. Fatty acid binding assay: using displacement of 8-anilinonaphthalene-1-sulfonic acid

Binding affinities of pFABPs to seven different fatty acids (DHA: docosahexaenoic acid; EPA: eicosapentaenoic acid; ALA: α-linolenic acid, linoleic acid, palmitic acid, oleic acid, and stearic acid) were determined using a Synergy MX Fluorescence Spectrophotometer (BioTek) at 293 K. ANS (1-anilino-8-naphthalene sulfonate) and fatty acids were dissolved in absolute ethanol and serially diluted with 20 mM Tris–HCl (pH 8.0) and 150 mM NaCl, with a final ethanol concentration not exceeding 1%. One milliliter of pFABP4 (1 μm) was equilibrated with ANS (50 μm) for 1 min. Displacement of ANS was measured by increasing the concentration of fatty acids. Fatty acids were added to the pFABPs-ANS complex and incubated 1 min for displacement and binding of ANS to pFABPs was monitored by excitation at 370 nm and emission at 475 nm.

2.3. Crystallization and data collection

Initial crystallization screening of apo-pFAPB4, pFABP4-linoleate complex, and pFABP5-palmitate complex were performed using commercially available crystallization solution kits: MCSG I-IV (Microlytic, Burlington, USA), Wizard Classic I-IV (Emerald Bio, Seattle, USA), and Classics and Classics II Suite (Qiagen, Hilden, Germany) with the sitting-drop vapor-diffusion method at 293 K in 96-well crystallization plates (Emerald Bio, Bainbridge Island, WA). Prior to crystallization, pFABPs were incubated with five-fold molar excess of each ligand overnight at 20 °C. Ligand stock solutions had a final concentration of 10 mM in 100% ethanol. Serially diluted fatty acids were added to the protein solution, so that the final concentration of ethanol did not exceed 1%. The crystallization drops consisted of 0.8 μl of protein with or without ligand solution and 0.8 μl of crystallization solution. The drop volume was increased from 0.8 μl to 1 μl using the hanging-drop vapor-diffusion method in 24-well plates. As a result, the crystal of pFABP4 was a hexagonal pyramid obtained from a solution of 0.2 M magnesium chloride, 0.1 M Tris (pH 8.3), and 27% (w/v) PEG 3350 at 293 K. The crystal of the pFABP4-linoleic acid complex was obtained from 0.1 M CHES (pH 9.5) and 30% (w/v) PEG 3000. The crystal of pFABP5-palmitate complex was obtained as a square pillar from 0.2 M magnesium chloride, 0.1 M Tris (pH 8.5) and 30% (w/v) PEG 4000. The optimized single crystals were harvested with cryoloop and protected from liquid-nitrogen gas stream using Paratone-N oil (Hampton Research, Aliso Viejo, USA). These data were collected using a BL-7A beam line in the Pohang Accelerator Laboratory (PAL; Pohang, Korea) and data sets were processed using the HKL-2000 program [27].

2.4. Structure determination and refinement

A data set of ligand-unbound pFABP4, linoleate-bound pFABP4 and palmitate-bound pFABP4 were collected at 2.1 Å, 2.2 Å and 2.3 Å resolution in space group $P6_1$, $P6_1$ and $P2_1$ respectively. Matthews coefficient [28] was used to determine the predicted number of molecules in the asymmetric unit and the crystal structure of pFABPs was determined with *MOLREP* [29] using the crystal structure of human adipocyte fatty acid binding protein (hFABP4) (PDB code 3Q6L; unpublished work) as a model. The final coordinate of the pFABP4 was used for molecular replacement of linoleate bound pFABP4 form. The coordinates of the human epidermal fatty acid binding protein (hFABP5)(PDB code 4LKP) [30] were used as a model for molecular replacement of pFABP5. Iterative rounds of manual model building and refinement were performed using REFMAC5, and COOT [31]. Data collection and refinement statistics are presented in Supplementary data, Table S1.

All figures were generated using *PyMOL* [32] and all coordinates generated were deposited in the Protein Data Bank with accession codes 5BVQ, 5BVS and 5BVT, respectively.

3. Results and discussion

3.1. Overall structure of apo-pFABP4, linoleate-complexed pFABP4, and palmitate-complexed pFABP5

The crystal structure of apo-pFABP4, linoleate-complexed pFABP4, and palmitate-complexed pFABP5 from gentoo penguin (*P. papua*) were determined at 2.1, 2.2, and 2.3 Å resolution, respectively (Fig. 1). apo-pFABP4 contains two polypeptide chains and 108 water molecules arranged as an asymmetric unit and with an overall topology composed of 10 anti-parallel β-strands and two α-helices (Fig. 1A and B). The canonical β-barrel structure is cylindrical in shape with an internal hydrophobic cavity composed of multiple nonpolar side chains. Two α-helices, located between β1 and β2, provide a U-shaped capping structure with a helix-turn-helix conformation. The U-shaped capping structure can exist both in an open and closed state and serves as a portal for fatty acid internalization [22] while also being involved in the protein–protein interaction between hFABP4 and JAK2 [23]. These results suggest that the capping region of FABPs is functionally important both for ligand binding and signal transfer via partner protein binding.

In the pFABP4-linoleate complex structure, one linoleate molecule is located within the cylindrical body (Fig. 1C). In addition to hydrophobic interactions, the carboxyl group of linoleate also forms hydrogen bonds with bound water molecule (W1, Fig. 2A and B). Analysis of the binding site indicates that the first oxygen of the carboxyl group of bound linoleate forms hydrogen bonds with the OH group of Y129 as well as with a water molecule (W1), which in turn forms hydrogen bonds with the NH_2 group of the R107 side chain (Fig. 2B). The second oxygen atom of the linoleate head group also forms hydrogen bonds with the OH group of Y129 and the NE atom of R127. The ligand-binding site in apo-pFABP4 is partially blocked by the side chain of Arg127 residue, which swings to accommodate the ligand in the linoleate-bound form (Fig. 2C).

The crystal structure of palmitate bound pFABP5 was determined to be very similar to pFABP4 and belongs to the space group $P2_1$ with one complex molecule in an asymmetric unit. The two proteins share 57% sequence identity with an overall r.m.s. deviation of 1.21 Å over 130 Cα atoms. By analytical size-exclusion chromatography, both purified pFABP4 and pFABP5 have shown apparent molecular weights compatible with that of a monomer (data not shown). Most FABPs behave as monomers, except hFABP5 that forms a domain-swapped dimer when complexed with a ligand inhibitor [7] and mouse FABP4 that dimerizes in solution [24]. These observations suggest that FABPs may have structural flexibility and undergo structural or oligomeric changes facilitating entry or exit of hydrophobic ligands.

3.2. Ligand-binding properties of pFABP4 and pFABP5

The ligand-binding specificity of pFABP4 and pFABP5 was determined by steady-state fluorescence spectroscopy titration. The binding affinities of seven chemically different fatty acids were monitored and compared by measuring the changes in the fluorescence of ANS (1-anilinonaphthalene-8-sulfonic acid) (Fig. 3) [20]. The results indicate that linoleate has the highest binding affinity to pFABP4, whereas relatively lower affinity to pFABP5 while, DHA shows the strongest affinity to pFABP5 and palmitate shows affinity for pFABP5. Next, we tried to obtain the structures of linoleate-complexed pFABP4 and palmitate-complexed pFABP5.

Structural superimposition of pFABP5-palmitate complex on pFABP4-linoleate complex revealed U-shaped conformation similarity of palmitate with linoleate in pFABP4. The biggest structural difference is in the β3–β4 loop region, suggesting greater mobility compared to other regions (Fig. 4A). The Phe57 residue located in this loop region plays an important role in nuclear import of mFABP4 [24]. Upon palmitate binding to pFABP5, the β3–β4 loop moves outwards by 4 Å compared to linoleate-complexed pFABP4 structure (Fig. 4A). Notably, the Phe60 residue (Phe58 in pFABP4) in the β3–β4 loop region has a flipped conformation in linoleate-complexed pFABP4 structure (Fig. 4B). Moreover, the Leu78 and Thr30 residues (Ala76 and Met32 in pFABP4) cause structural changes to bound palmitate in pFABP5 compared to linoleate-complexed pFABP4. In palmitate-bound pFABP5, the Leu78 residue extends into the hydrophobic core resulting in hydrophobic interaction with palmitate. In the pFABP4-linoleate complex, however, the Leu78 is replaced by less bulky Ala76 residue increasing the volume of the internal hydrophobic cavity.

A comparison of the binding sites revealed that palmitate has a more extended conformation and is pushed aside from the center of internal pocket towards the α1-α2 capping region as compared to the bound linoleate in pFABP4 (Fig. 4B). Thus, the palmitate forms different and weak hydrogen bonds than linoleate around the hydrophilic carboxyl head group. In the pFABP5-palmitate complex, the carboxyl O atoms of the palmitate form water mediated hydrogen bonds with Tyr132 (Fig. 4C) while, the carboxyl O_2 atom of bound linoleate forms two hydrogen bonds with NE atom of Arg127 and OH atom of Tyr129 in pFABP4 (Fig. 4D). The other carboxyl O atom of linoleate forms water mediated hydrogen bonds with NH_2 atom of Arg107 and NE atom of Arg107 in linoleate bound-pFABP4.

Taken together, these results suggest that the ligand-binding modes and ligand-binding affinities of pFABP4 and pFABP5 are largely different. Therefore, several non-conserved residues can induce a significant space change in the ligand-binding site, and these variations may account for the fatty acid target specificities described in Fig. 3.

3.3. Comparison of the linoleate binding pocket between pFABP4 and mFABP4

The superimposition of pFABP4-linoleate complex with the mFABP4-linoleate complex (PDB code 2Q9S) [24] revealed that while the overall U-shaped structure of the bound linoleate is similar, the main difference lies in the V41/M40, L24/V23, and T57/T56 residues (underlining indicates pFABP4 residues) (Supplementary data, Fig. S1A). The W1 position of the pFABP4-linoleate complex contains the M40 residue in the mFABP4-linoleate complex thus, mFABP4 does not exhibit W1 mediated hydrogen bond interaction. However, mFABP4 still has a conserved

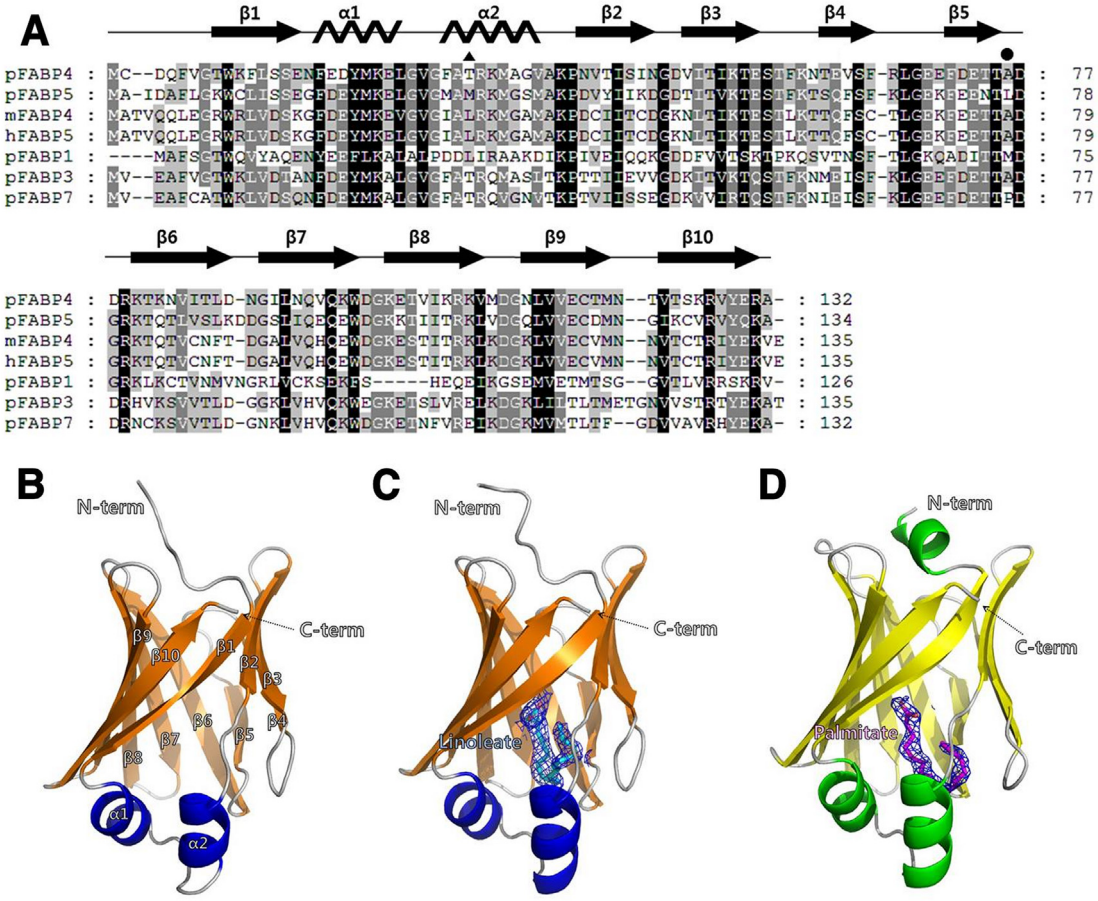

Fig. 1. Sequence alignment and crystal structure of pFABPs (A) Multiple sequence alignment of pFABPs from gentoo penguin (*Pygoscelis papua*). The secondary structural elements in the crystal structure of pFABP4 are represented above the multiple sequence alignment. The Thr30 residue is represented by a black triangle and Ala76 residue is represented by a filled circle. (B) Schematic representation of the overall structure of ligand-unbound pFABP4. β-strands (β1–β10) and α helices (α1 and α2) along with numbering of secondary structure elements are shown. The α-helices are in blue and β-strands are in orange. (C) Ribbon representation of the linoleate-bound pFABP4 structure. The bound linoleate molecule is shown as a cyan stick model with a 2Fo-Fc electron density map (contoured at 1σ). (D) Ribbon representation of the palmitate-bound pFABP5 structure. The bound palmitate molecule is shown as a magenta stick model with a 2Fo-Fc electron density map (contoured at 1σ).

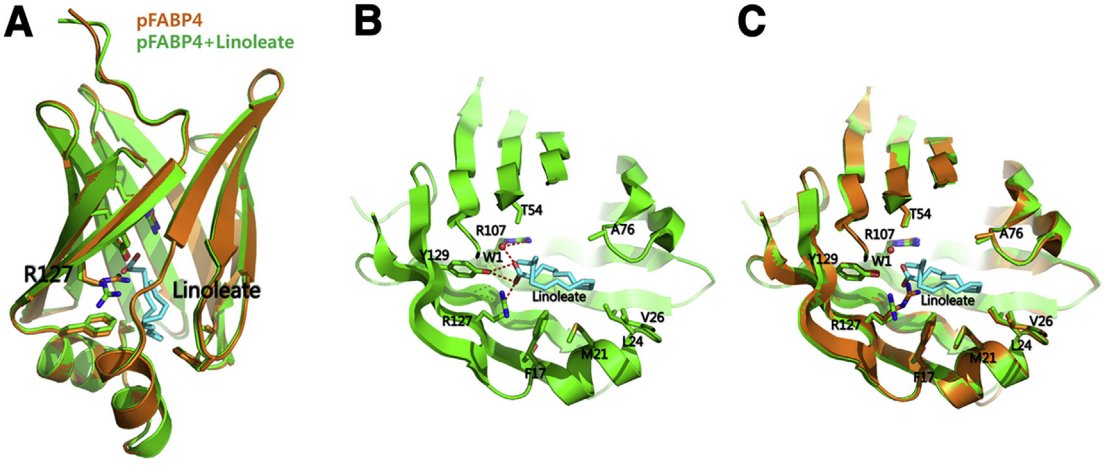

Fig. 2. Structural comparison of ligand-unbound pFABP4 and linoleate-bound pFABP4. (A) Structural superimposition of pFABP4 ligand free-form (orange) and linoleate-bound form (green). (B) The linoleate-binding site of pFABP4. The side chains of the residues in the vicinity of the bound linoleate are indicated by sticks. Hydrogen bond interactions between the carboxyl head group of linoleate and pFABP4 are shown with red dashed lines. The carbon tail of linoleate forms hydrophobic interactions with Phe17, Met21, Leu24, Val26 and Ala76. (C) A magnified view of the ligand-binding pocket with the surrounding residues from the superimposed apo-pFABP4 (orange) and linoleate-bound pFABP4 (green) structures.

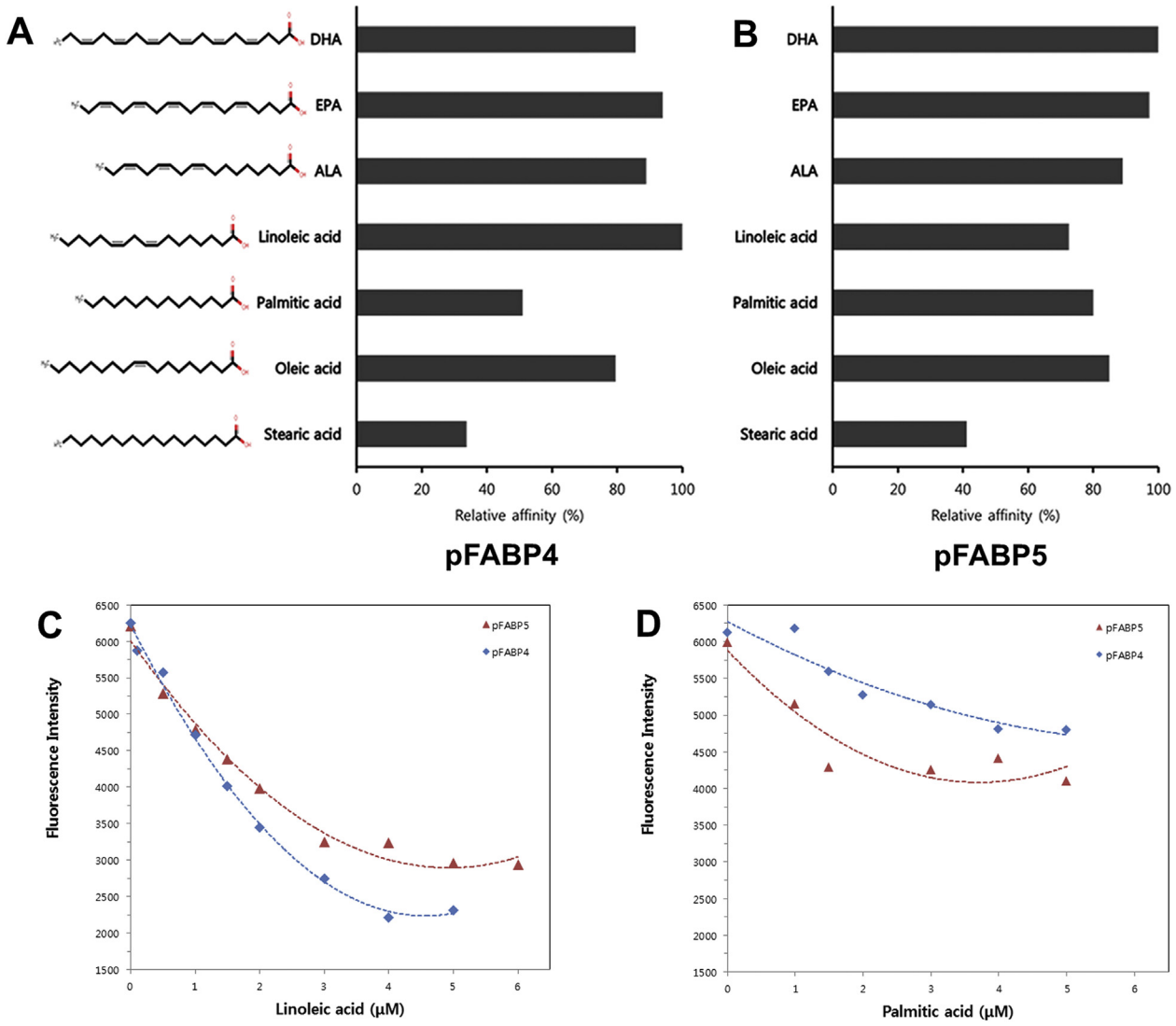

Fig. 3. Ligand-binding properties of pFABP4 and pFABP5. (A) This graph compares the binding affinities of the fatty acid ligands to pFABP4. The percent binding is expressed relative to the binding of linoleate to pFABP4 (100%). (B) This graph compares the binding affinities of the fatty acid ligands to pFABP5. The percent binding is expressed relative to the binding of DHA to pFABP5 (100%). (C) Comparison of linoleic acid affinities of pFABP4 and pFABP5. (D) Comparison of palmitic acid affinities of pFABP4 and pFABP5.

polar interaction with the head carboxyl group of linoleate at residues Y128 and R126. The L24 residue in pFABP4 pushes the bound linoleate molecule in the opposite direction, producing a slightly different linoleate conformation compared to mFABP4-linoleate complex. Another major structural difference exists in the loop region between β3 and β4. The T56 residue in the mFABP4-linoleate complex has a flipped peptide bond, oriented toward the outside of the core structure. These differences result in a smaller cavity volume (about 100 $Å^3$) in mFABP4 compared to pFABP4. The calculated cavity volumes of representative FABPs are listed in Supplementary data, Table S2. Notably, hFABP1 (PDB code 3STN) has the largest cavity volume, allowing for multi-ligand binding [25]. In contrast, pFABP5 has the smallest cavity volume because of the inward protrusion of L78 residue (Supplementary data, Table S2).

3.4. Comparison of the palmitate binding pocket between pFABP5 and hFABP5

The structural superimposition of the pFABP5-palmitate complex with the hFABP5-palmitate complex (PDB code 1B56) [26] shows that while the FABP molecules overlap very well the bound palmitate has different binding interactions and positions. The most striking difference is in the binding position of palmitate in the hydrophobic cavity that exhibits higher number of hydrogen interactions compared to pFABP5. The carboxyl group of palmitate migrates deep into the cavity making hydrogen bonds with Arg109, Arg129 and Tyr131. While, only four residues are different between the ligand binding pocket of pFABP5 and hFABP5 (Val43/Cys43, Ser63/Thr63, Leu78/Ala78 and Phe69/Leu60 for pFABP5/hFABP5, respectively), the major differences in the bound palmitate are due to Leu78 (corresponding to Ala78 in hFABP5). The side chain of Leu78 pushes the bound palmitate opposite to the α2-helix direction contributing to its different conformation (Supplementary data, Fig. S1B).

In summary, X-ray crystallography and structural comparisons, combined with a ligand-binding assay, provide important insights into the mechanism behind the ligand specificities of pFABP4 and pFABP5.

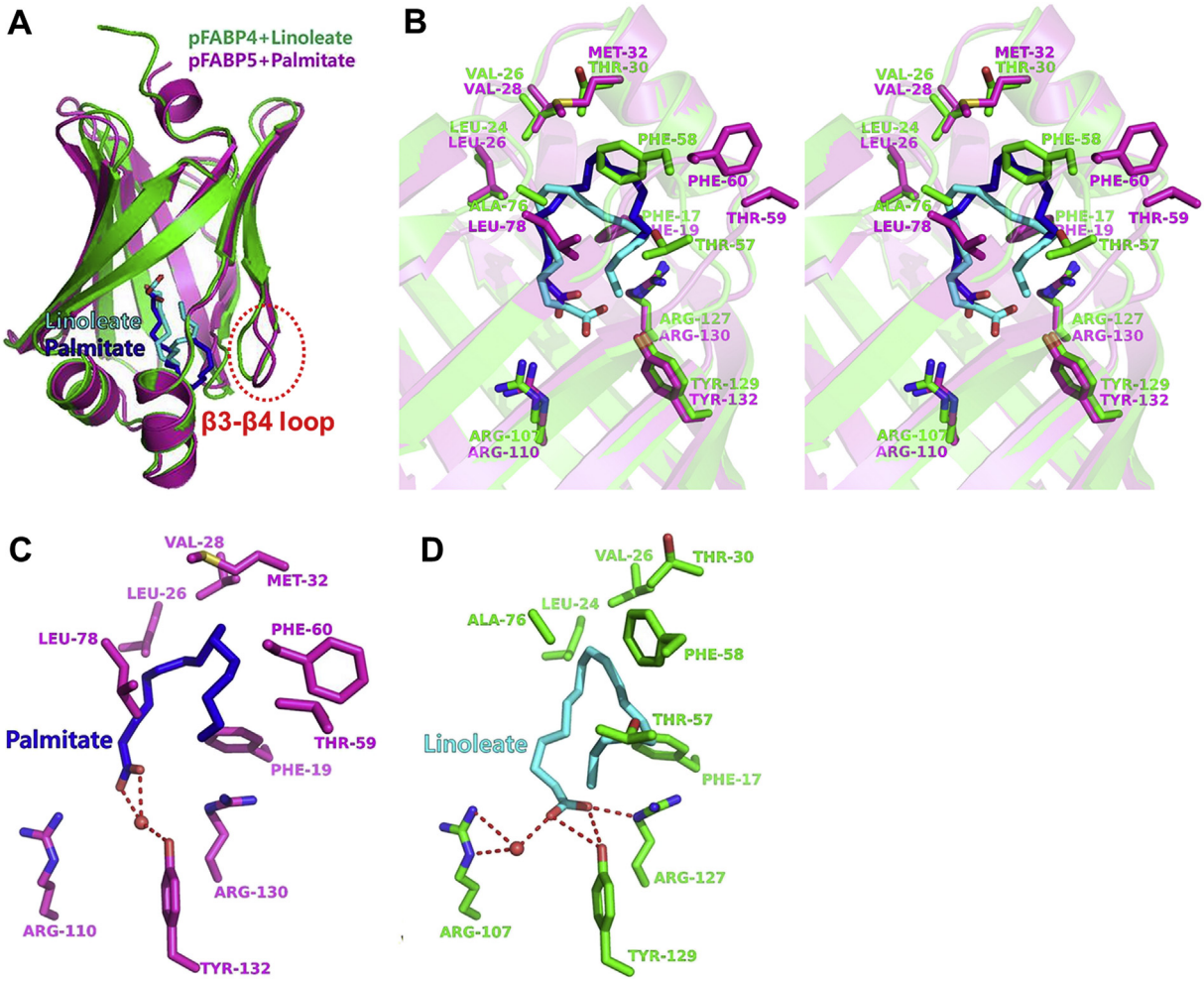

Fig. 4. Ligand-binding mode in pFABP4 and pFABP5. (A) The structural superimposition of linoleate(cyan)-bound pFABP4 and palmitate(blue)-bound pFABP5 (magenta) reveals a conformational change in the β3–β4 loop region. (B) Stereo view of the superimposed structures of linoleate(cyan)-bound pFABP4 and palmitate(blue)-bound pFABP5 (magenta). (C) The palmitate binding mode and interacting residues in pFABP5 are shown as a stick model. The hydrogen bonds are shown as red dashes. (D) The linoleate binding mode and detailed interactions with pFABP4 are shown as a stick model. Color codes are the same as Fig. 2B.

Acknowledgments

We would like to thank the staff at the X-ray core facility of Korea Basic Science Institute (KBSI) (Ochang, Korea) and BL-7A of the Pohang Accelerator Laboratory (Pohang, Korea) for their kind help with data collection. This research was supported by a grant for the project titled “Korea-Polar Ocean Development: K-POD” (project no. PM14050) funded by the Ministry of Oceans and Fisheries, Korea and this work was also supported by the Antarctic organisms: Cold-Adaptation Mechanisms and its application grant (PE15070) funded by the Korea Polar Research Institute and Basic Science Research Program through the National Research Foundation of Korea (NRF) funded by the Ministry of Education, Science and Technology to JHC (2013R1A1A1061391).

Appendix A. Supplementary data

Supplementary data related to this article can be found at http://dx.doi.org/10.1016/j.bbrc.2015.07.087.

Transparency document

Transparency document related to this article can be found online at http://dx.doi.org/10.1016/j.bbrc.2015.07.087.

References

[1] M. Furuhashi, G.S. Hotamisligil, Fatty acid-binding proteins: role in metabolic diseases and potential as drug targets, Nat. Rev. Drug Discov. 7 (2008) 489–503.
[2] A. Chmurzyńska, The multigene family of fatty acid-binding proteins (FABPs): function, structure and polymorphism, J. Appl. Genet. 47 (2006) 39–48.
[3] R.K. Ockner, J.A. Manning, R.B. Poppenhausen, W.K. Ho, A binding protein for fatty acids in cytosol of intestinal mucosa, liver, myocardium, and other tissues, Science 177 (1972) 56–58.
[4] J. Storch, A.E. Thumser, Tissue-specific functions in the fatty acid-binding protein family, J. Biol. Chem. 285 (2010) 32679–32683.
[5] J. Storch, L. McDermott, Structural and functional analysis of fatty acid-binding proteins, J. Lipid Res. 50 (2009) S126–S131.
[6] S. Matsuoka, S. Sugiyama, D. Matsuoka, M. Hirose, S. Lethu, H. Ano, T. Hara, O. Ichihara, S.R. Kimura, S. Murakami, Water-mediated recognition of simple alkyl chains by heart-type fatty-acid-binding protein, Angew. Chem. Int. Ed. 54 (2014) 1508–1511.
[7] B. Sanson, T. Wang, J. Sun, L. Wang, M. Kaczocha, I. Ojima, D. Deutsch, H. Li, Crystallographic study of FABP5 as an intracellular endocannabinoid transporter, Acta Crystallogr. Sect. D. Biol. Crystallogr. 70 (2014) 290–298.
[8] G. Scapin, P. Spadon, M. Mammi, G. Zanotti, H.L. Monaco, Crystal structure of chicken liver basic fatty acid-binding protein at 2.7 Å resolution, Mol. Cell. Biochem. 98 (1990) 95–99.
[9] S. Capaldi, G. Saccomani, D. Fessas, M. Signorelli, M. Perduca, H.L. Monaco, The X-ray structure of zebrafish (Danio rerio) ileal bile acid-binding protein reveals the presence of binding sites on the surface of the protein molecule, J. Mol. Biol. 385 (2009) 99–116.
[10] J.A. Hamilton, Fatty acid interactions with proteins: what X-ray crystal and NMR solution structures tell us, Prog. Lipid Res. 43 (2004) 177–199.
[11] G. Zanotti, L. Feltre, P. Spadon, A possible route for the release of fatty acid

from fatty acid-binding protein, Biochem. J. 301 (1994) 459–463.
[12] L. Gutierrez-Gonzalez, C. Ludwig, C. Hohoff, M. Rademacher, T. Hanhoff, H. Ruterjans, F. Spener, C. Lucke, Solution structure and backbone dynamics of human epidermal-type fatty acid-binding protein (E-FABP), Biochem. J. 364 (2002) 725–737.
[13] J. Storch, A.E. Thumser, The fatty acid transport function of fatty acid-binding proteins, Biochim. Biophys. Acta (BBA) Mol. Cell Biol. Lipids 1486 (2000) 28–44.
[14] J. Cai, C. Lücke, Z. Chen, Y. Qiao, E. Klimtchuk, J.A. Hamilton, Solution structure and backbone dynamics of human liver fatty acid binding protein: fatty acid binding revisited, Biophys. J. 102 (2012) 2585–2594.
[15] F. Angelucci, K.A. Johnson, P. Baiocco, A.E. Miele, M. Brunori, C. Valle, F. Vigorosi, A.R. Troiani, P. Liberti, D. Cioli, Schistosoma mansoni fatty acid binding protein: specificity and functional control as revealed by crystallographic structure, Biochemistry 43 (2004) 13000–13011.
[16] R. Patil, A. Laguerre, J. Wielens, S.J. Headey, M.L. Williams, M.L. Hughes, B. Mohanty, C.J. Porter, M.J. Scanlon, Characterization of two distinct modes of drug binding to human intestinal fatty acid binding protein, ACS Chem. Biol. 9 (2014) 2526–2534.
[17] M.H. Fenner, E. Elstner, Peroxisome proliferator-activated receptor-γ ligands for the treatment of breast cancer, Expert Opin. Investig. Drugs 14 (2005) 557–568.
[18] N.-S. Tan, N.S. Shaw, N. Vinckenbosch, P. Liu, R. Yasmin, B. Desvergne, W. Wahli, N. Noy, Selective cooperation between fatty acid binding proteins and peroxisome proliferator-activated receptors in regulating transcription, Mol. Cell. Biol. 22 (2002) 5114–5127.
[19] D. Dong, S.E. Ruuska, D.J. Levinthal, N. Noy, Distinct roles for cellular retinoic acid-binding proteins I and II in regulating signaling by retinoic acid, J. Biol. Chem. 274 (1999) 23695–23698.
[20] C.D. Kane, D.A. Bernlohr, A simple assay for intracellular lipid-binding proteins using displacement of 1-anilinonaphthalene 8-sulfonic acid, Anal. Biochem. 233 (1996) 197–204.
[21] J.J. Ory, L.J. Banaszak, Studies of the ligand binding reaction of adipocyte lipid binding protein using the fluorescent probe 1, 8-anilinonaphthalene-8-sulfonate, Biophys. J. 77 (1999) 1107–1116.
[22] F.M. Herr, J. Aronson, J. Storch, Role of portal region lysine residues in electrostatic interactions between heart fatty acid binding protein and phospholipid membranes, Biochemistry 35 (1996) 1296–1303.
[23] B.R. Thompson, A.M. Mazurkiewicz-Muñoz, J. Suttles, C. Carter-Su, D.A. Bernlohr, Interaction of adipocyte fatty acid-binding protein (AFABP) and Jak2 AFABP/AP2 as a regulator of Jak2 signaling, J. Biol. Chem. 284 (2009) 13473–13480.
[24] R.E. Gillilan, S.D. Ayers, N. Noy, Structural basis for activation of fatty acid-binding protein 4, J. Mol. Biol. 372 (2007) 1246–1260.
[25] A. Sharma, A. Sharma, Fatty acid induced remodeling within the human liver fatty acid-binding protein, J. Biol. Chem. 286 (2011) 31924–31928.
[26] C. Hohoff, T. Börchers, B. Rüstow, F. Spener, H. van Tilbeurgh, Expression, purification, and crystal structure determination of recombinant human epidermal-type fatty acid binding protein, Biochemistry 38 (1999) 12229–12239.
[27] Z. Otwinowski, W. Minor, Processing of X-ray diffraction data, Methods Enzymol. 276 (1997) 307–326.
[28] B.W. Matthews, Solvent content of protein crystals, J. Mol. Biol. 33 (1968) 491–497.
[29] A. Vagin, A. Teplyakov, MOLREP: an automated program for molecular replacement, J. Appl. Crystallogr. 30 (1997) 1022–1025.
[30] E.H. Armstrong, D. Goswami, P.R. Griffin, N. Noy, E.A. Ortlund, Structural basis for ligand regulation of the fatty acid-binding protein 5, peroxisome proliferator-activated receptor β/δ (FABP5-PPARβ/δ) signaling pathway, J. Biol. Chem. 289 (2014) 14941–14954.
[31] P. Emsley, K. Cowtan, Coot: model-building tools for molecular graphics, Acta Crystallogr. Sect. D Biol. Crystallogr. 60 (2004) 2126–2132.
[32] W.L. DeLano, The PyMOL Molecular Graphics System, 2002.